Geophysical Research Letters

RESEARCH LETTER
10.1029/2017GL076498

Key Points:
- Differing choices of depth horizon commonly used to define export flux yield widely varying global rates and efficiencies of export
- Zonal variability in POC flux and e-ratio is more pronounced when evaluated at the euphotic depth than at the maximum annual MLD
- POC flux and e-ratio estimates in subpolar regions with deep winter mixing are especially sensitive to the choice of export depth horizon

Supporting Information:
- Supporting Information S1

Correspondence to:
H. I. Palevsky,
hpalevsky@whoi.edu

Citation:
Palevsky, H. I., & Doney, S. C. (2018). How choice of depth horizon influences the estimated spatial patterns and global magnitude of ocean carbon export flux. *Geophysical Research Letters, 45*, 4171–4179. https://doi.org/10.1029/2017GL076498

Received 20 NOV 2017
Accepted 12 APR 2018
Accepted article online 23 APR 2018
Published online 5 MAY 2018

How Choice of Depth Horizon Influences the Estimated Spatial Patterns and Global Magnitude of Ocean Carbon Export Flux

Hilary I. Palevsky[1] **and Scott C. Doney**[2]

[1]Department of Marine Chemistry and Geochemistry, Woods Hole Oceanographic Institution, Woods Hole, MA, USA, [2]Department of Environmental Sciences, University of Virginia, Charlottesville, VA, USA

Abstract Estimated rates and efficiency of ocean carbon export flux are sensitive to differences in the depth horizons used to define export, which often vary across methodological approaches. We evaluate sinking particulate organic carbon (POC) flux rates and efficiency (e-ratios) in a global earth system model, using a range of commonly used depth horizons: the seasonal mixed layer depth, the particle compensation depth, the base of the euphotic zone, a fixed depth horizon of 100 m, and the maximum annual mixed layer depth. Within this single dynamically consistent model framework, global POC flux rates vary by 30% and global e-ratios by 21% across different depth horizon choices. Zonal variability in POC flux and e-ratio also depends on the export depth horizon due to pronounced influence of deep winter mixing in subpolar regions. Efforts to reconcile conflicting estimates of export need to account for these systematic discrepancies created by differing depth horizon choices.

Plain Language Summary The ocean's carbon cycle is strongly influenced by tiny marine plants that transform carbon dioxide into organic carbon in the surface ocean. A fraction of this organic matter sinks into the deep ocean as decomposing dead organisms, storing their carbon away from contact with the atmosphere. Researchers studying this process often select different depths that dead organisms must sink below in order to be counted in their analyses. This can make it difficult to compare across different studies to determine how much sinking organic matter is leaving the surface ocean. In this study, we compare results across many of the different depth choices often used by researchers. Since there are not sufficient observations to compare globally across all these depths, our analysis uses a global model simulating the ecosystem processes that produce sinking organic matter. We show that researchers' conclusions about the global rate and efficiency of organic carbon transfer out of the surface ocean, as well as the relative contributions of different ocean regions, depend heavily on this choice of how deep organic matter must sink in order to be counted. This has important implications for how researchers study biology's role in the modern and future ocean carbon cycle.

1. Introduction

Export of biologically fixed organic carbon from the surface ocean plays an important role in the global carbon cycle, with significant implications for the ocean's role in regulating global climate and for ocean acidification and deoxygenation. Earth system model projections indicate that export flux will decrease over the 21st century (Bopp et al., 2013; Laufkötter et al., 2016), but there is significant uncertainty in these estimates due in part to uncertainty in our ability to quantify the global magnitude and spatial patterns of export in today's ocean. Current estimates of global export flux vary widely, ranging from 5 to 13 Pg C/year (Laws, D'Sa, & Naik, 2011; Siegel et al., 2014, 2016). Estimates of spatial patterns of export also vary, with satellite algorithms and models showing higher export in subpolar than in subtropical regions, while geochemical mass balance approaches indicate more globally uniform rates (Emerson, 2014).

The wide variety of methods to measure export in the modern ocean provide both an opportunity to more accurately assess export and a confounding factor in comparing results from different studies. Direct observational techniques to assess export include geochemical mass balance (oxygen, carbon, and nitrogen), incubation experiments to determine "new" production from nitrate, and assessment of particle flux rates based on ^{234}Th disequilibrium measurements, collection of particles in sediment traps, and emerging autonomous optical techniques (Buesseler et al., 1992, 2007; Emerson, 2014; Emerson & Hedges, 2008; Estapa et al., 2017). These direct observational estimates have been extrapolated to a global scale by using them to constrain remote sensing algorithms (Dunne et al., 2005, 2007; Henson et al., 2011; Laws et al., 2000, 2011;

Siegel et al., 2014). Applying a wide array of methods confers an advantage in accurately constraining export despite uncertainties inherent to each individual method. However, a complication that plagues comparisons among studies is that differing approaches to measure export often differ in how export is defined. For example, previous work has highlighted discrepancies in export estimates that span different temporal or spatial scales or include different mechanisms of export (sinking particles, physical transport of suspended or dissolved material, and/or active transport by zooplankton; e.g., Emerson, 2014; Estapa et al., 2015; Hansell & Carlson, 1998; Siegel et al., 2016; Stange et al., 2017; Steinberg et al., 2000; Steinberg & Landry, 2017).

An additional key difference among methods that has received insufficient attention is that there is no consistent choice of the depth horizon below which organic carbon must sink to be counted as exported. Observational studies of sinking particle fluxes often evaluate export at the base of the euphotic zone, approximating the depth below which new particles are not produced (Buesseler & Boyd, 2009; Siegel et al., 2016). Mass balance estimates of net community production (equivalent to export when in steady state) commonly evaluate export at the base of the seasonally varying mixed layer or annual net community production at the maximum annual mixed layer depth (MLD) to only include material that will be sequestered from the atmosphere on annual or longer timescales (Emerson, 2014). Modeling studies have long acknowledged that estimates of export are sensitive to the choice of depth horizon but have still generally chosen a single constant global depth horizon to facilitate global-scale analysis (e.g., Doney et al., 2003; Laufkötter et al., 2016; Najjar et al., 2007).

These different choices of depth horizon to evaluate export reflect not only technical differences among methods that lend themselves to certain depth horizon choices but also differences in the driving scientific questions. For instance, evaluating export at the base of the euphotic zone separates overlying processes that produce organic carbon from the region below where only remineralization occurs, making it an ideal choice to assess energy sources for the mesopelagic or food web dynamics influencing export (e.g., Buesseler & Boyd, 2009). A similar justification holds for evaluating export at the compensation depth (where net production and remineralization are equal, with net production above and net remineralization below, sensu Najjar & Keeling, 1997), although this is rarely applied observationally due to challenges of identifying the compensation depth in the field. For questions connecting export to the ocean carbon sink, it is valuable to consider the physical dynamics controlling CO_2 exchange between the ocean and atmosphere. The seasonal MLD is a natural depth horizon choice to evaluate the mechanistic connection between export and atmospheric pCO_2, since export drives air-sea CO_2 flux by altering mixed layer pCO_2. A key additional factor in understanding the influence of export on the carbon cycle is the timescale over which exported material is sequestered from contact with the atmosphere, which depends on both seasonal mixing and large-scale circulation (e.g., DeVries et al., 2012). Prior observational studies have demonstrated that a significant fraction of the carbon exported from the surface ocean during the stratified summer months can be ventilated during deep winter mixing, such that the maximum annual MLD is the ideal depth horizon to assess how export sequesters carbon on annual or longer timescales (Körtzinger et al., 2008; Palevsky, Quay, Lockwood, et al., 2016). While each of these depth horizon choices has clear utility, comparing findings among studies using these different definitions of export can be challenging. It is clear that different depth horizon choices will lead to differing estimates of the rate and efficiency of export due to rapid attenuation of export flux with depth (Martin et al., 1987), but systematic effects of differing choices of export depth horizon have not been evaluated on a global scale.

In this paper, we use output from a biogeochemical ocean model to compare export rates and efficiencies evaluated at multiple depth horizons, selected to represent a range of choices commonly used to define export in observational and modeling studies (Table 1). By comparing results across depth horizons within a single dynamically consistent model framework, we demonstrate the influence of the choice of depth horizon used to define export on calculated global rates and spatial patterns of export flux and efficiency. We find that these discrepancies are most pronounced in regions that experience deep winter mixing, particularly the subpolar regions, such that the choice of export depth horizon influences conclusions about spatial patterns as well as global rates of export. Based on these findings, we provide recommendations for future observational and modeling studies to clearly specify the choice of export horizon for a given analysis and, wherever possible, present profiles of export flux and efficiency across multiple depth horizons in order to improve intercomparison among studies using different definitions of export.

Table 1
Depth Horizons Used to Define Export and Global Model Results at Each Depth Horizon

Depth horizon	Depth horizon definition for CCSM-BEC analysis	Methods commonly using this depth horizon	Global POC flux from CCSM-BEC (Pg C/year)	Global e-ratio from CCSM-BEC (%)
Seasonally varying MLD	From model physics, determined for each grid point in each month	Biogeochemical mass balance (e.g., O_2, NO_3, and DIC), especially over short timescales	5.3	14.6
Particle compensation depth	Depth through the water column with the maximum POC flux rate, determined for each grid point in each month	Rarely applied observationally	6.9	14.5
Euphotic depth	Depth where POC production = 1% of the maximum through the water column (as defined by Lima et al., 2014), determined for each grid point in each month	Sediment trap and ^{234}Th observational studies; satellite e-ratio algorithms	6.0	12.4
100 m	Constant for all grid points and months	Earth system models; sediment trap and ^{234}Th observational studies	6.2	12.9
Maximum annual MLD	From model physics, determined for each grid point and constant throughout a year	Biogeochemical mass balance (O_2 and O_2/Ar), especially over annual and longer timescales	5.6	12.1

Note. Further details about how these depth horizons are calculated from CCSM-BEC output are provided in the supporting information. DIC = dissolved inorganic carbon; MLD = mixed layer depth; POC = particulate organic carbon. CCSM-BEC = Community Climate System Model with the Biogeochemical Elemental Cycle module.

2. Methods

The analysis presented here could be conducted using any global ocean model that provides realistic depth- and time-resolved rates of primary production and organic carbon flux. However, standard runs for previous model intercomparison projects (e.g., Taylor et al., 2012) have not routinely archived the depth-resolved output needed for such an analysis and instead only provide organic carbon flux at the 100-m-depth horizon. We therefore use depth- and time-resolved model output previously published and evaluated by Lima et al. (2014), from a preindustrial control simulation of the Community Climate System Model run with an embedded biogeochemistry and ecosystem module (the Biogeochemical Elemental Cycle model; Moore et al., 2004). The model includes three phytoplankton functional groups, a single adaptive zooplankton class, and multielement (N, P, Si, and Fe) limitation of phytoplankton growth. Particulate organic carbon (POC) is produced by large phytoplankton aggregation, mortality of both phytoplankton and zooplankton, and zooplankton grazing on phytoplankton. POC sinking and remineralization rates are treated implicitly, with POC flux attenuation determined using a variable remineralization length scale (ranging from 150 to 330 m) that depends on particle composition and environmental conditions, yielding POC flux profiles that correspond reasonably well with observational measurement profiles (Figure S1 in the supporting information; Buesseler & Boyd, 2009; Marsay et al., 2015; for global comparison between modeled POC flux and sediment trap measurements, see Lima et al., 2014). The version of the model used here provides 3.6° longitude × 0.8° to 1.8° latitude resolution, with 25 vertical levels, and we use a monthly climatology created from the final 10 years of an 840-year simulation run with a repeated annual cycle of physical forcing derived from atmospheric reanalysis and satellite data products and preindustrial atmospheric CO_2 concentrations (280 ppmv; Lima et al., 2014).

Our analysis focuses on POC flux as a key component of export and on the fraction of net primary production (NPP) that contributes to POC flux (the e-ratio; POC flux/NPP), a metric of export efficiency. NPP at each depth represents total NPP from all three phytoplankton groups integrated through the overlying water column, and POC flux represents sinking POC at each depth (i.e., the difference between POC production and remineralization integrated through the overlying water column). Both POC flux and e-ratio in the model output are four-dimensional properties that vary with time, space, and depth. To compute annual POC flux rates and e-ratios for each latitude × longitude grid cell, we define a set of depth horizons based on depths commonly used to assess export observationally and in model analyses (Table 1). Some of these depth horizons are a single fixed depth for all months (100 m and maximum annual MLD), while others change seasonally

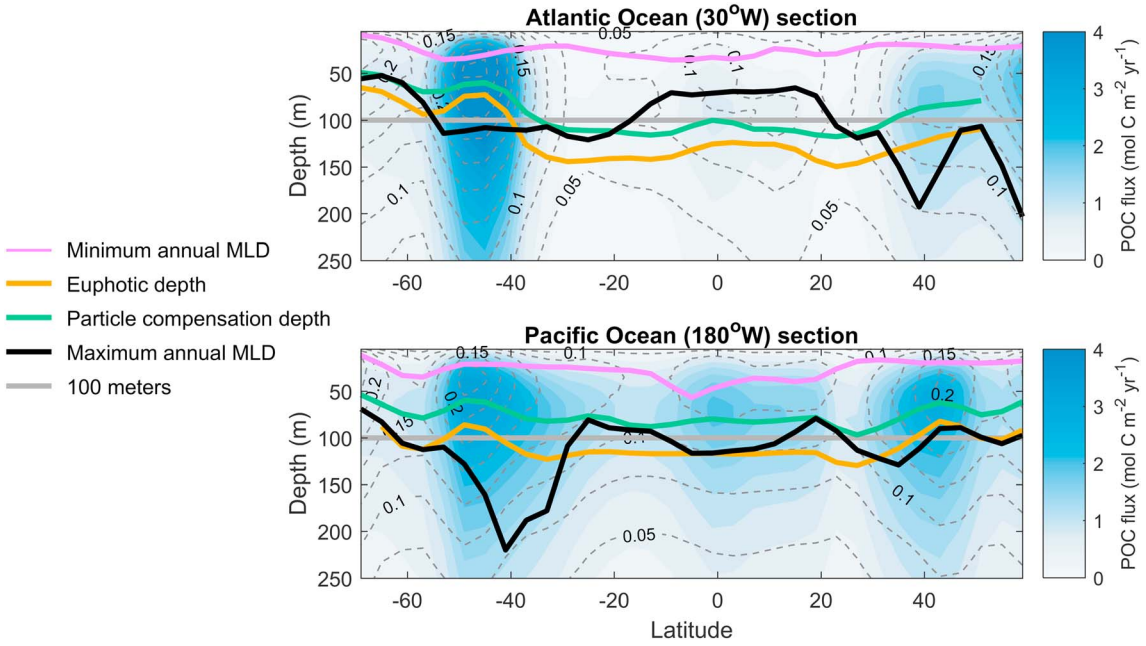

Figure 1. Meridional sections of mean annual POC flux (colorscale) and e-ratio (POC flux/net primary production; dashed gray lines) in the Atlantic (top) and Pacific (bottom) Oceans. Five different depth horizons used for defining export are shown in the solid colored lines. For the particle compensation depth and euphotic depths, which vary seasonally, the depth shown is the annual mean weighted by monthly POC flux rates. The seasonal MLD export horizon varies between the annual minimum (pink) and maximum (black). MLD = mixed layer depth; POC = particulate organic carbon.

(seasonally varying MLD, particle compensation depth, and euphotic depth; Figure S2). Annual rates are calculated using climatological monthly output evaluated at the suite of month-specific depth horizons (see supporting information for further details).

We acknowledge that the model's POC production and remineralization dynamics are simplistic as compared with the real world, but they nonetheless represent realistic POC flux profiles (Figure S1; Lima et al., 2014) and therefore enable us to investigate global-scale trends and identify regions that merit further observational attention to the choice of export depth horizon. The model output analyzed here includes POC flux but does not include transport of dissolved organic carbon (DOC) or vertical transport by zooplankton. This analysis therefore focuses solely on export by POC flux, but we acknowledge that DOC and zooplankton export are also key components of organic carbon export (Hansell & Carlson, 1998; Roshan & DeVries, 2017; Steinberg & Landry, 2017) and that the sensitivity of these mechanisms to the choice of depth horizon merits analysis in future work.

3. Results and Discussion

3.1. Model POC Flux and e-Ratio

Modeled POC flux and e-ratio patterns through the upper water column are illustrated in sections from both the Atlantic and Pacific Oceans (Figure 1). POC flux is low at the surface and increases with depth through the uppermost water column where POC production exceeds remineralization (i.e., above the particle compensation depth). Below the particle compensation depth, POC flux decreases with depth as sinking particles are remineralized (global mean of 80% ± 8% remineralized in the first 100 m below the compensation depth). The model's global mean particle compensation depth is 75 ± 20 m, with shallower (deeper) compensation depths found in regions with higher (lower) POC flux. The euphotic depth is consistently slightly deeper than the particle compensation depth (29 ± 10 m deeper), since remineralization exceeds production at the lower production rates in the deepest portion of the euphotic zone.

The e-ratio shows a similar pattern to POC flux with depth, but the maximum e-ratio through the water column is displaced closer to the surface than for POC flux (Figure 1). This is consistent with previous analysis of

Biogeochemical Elemental Cycle model output, which showed photosynthesis rates dropping off more steeply than respiration rates with depth, yielding maximum e-ratios near the surface (Palevsky, Quay, & Nicholson, 2016). As a result, the model yields higher e-ratios at the stratified summertime MLD than the particle compensation depth (which is by definition the maximum POC flux of all possible depth horizons). Analysis of a single earth system model cannot determine whether this relationship between the depths of maximum e-ratio and POC flux in the model reflects a phenomenon in the real ocean but does indicate that care and consistency are especially needed in selecting depth horizons used to evaluate export rates and e-ratios in tandem due to the likelihood of their maxima being displaced in the water column.

3.2. Relationship Between Winter Mixing Depth and POC Flux

The significance of different choices for export depth horizon is particularly evident for locations that experience deep winter mixing. While the euphotic and particle compensation depths are based on biological dynamics, the seasonal and maximum annual MLD depth horizons are based on physical dynamics of seasonally variable stratification. Simulated MLDs generally match observed trends (for a detailed comparison with observations, see Doney et al., 2009). Minimum annual mixed layers (24 ± 14 m), occurring during the summer-stratified season, are relatively uniform globally. Some regions maintain strong year-round stratification, while others experience strong winter mixing that produces a wider range of seasonal MLDs and deeper maximum annual MLDs. The deepest winter mixed layers are generally found in the subpolar latitudes (30°–60°), in the Southern Ocean, the Kuroshio region of the western North Pacific, and the subpolar North Atlantic (Figure 2a). In these regions, the maximum annual MLD is substantially deeper than the other commonly used export depth horizons, allowing remineralization below the other depth horizons but above the maximum annual MLD to significantly attenuate the POC flux.

To illustrate the influence of deep winter mixing on differences among export depth horizons, we compare annual POC flux evaluated globally at both the maximum annual MLD and the fixed 100-m depth horizon commonly used in prior model analyses (Figures 2b and 2c). Regions in red in Figure 2b indicate net remineralization of POC between 100 m and the maximum annual MLD, with the difference representing sinking organic material that is counted as exported using the fixed 100-m depth horizon but is subsequently remineralized and ventilated during winter mixing and therefore not counted as exported using the maximum annual MLD horizon. Regions experiencing the deepest winter mixing show the most pronounced decrease in POC flux when evaluated at the maximum annual MLD rather than the 100-m depth horizon, with aggregated data from all model grid cells illustrating the correlation between maximum annual MLD and the discrepancy between POC flux determined at these two different export depth horizons (Figure 2c). Note that for some regions with strong year-round stratification, the maximum annual MLD is $<$100 m, such that POC flux at the maximum annual MLD can be greater than at 100 m due to net POC remineralization below the maximum annual MLD and above 100 m.

It is striking that although differences in POC flux evaluated at different depth horizons are also influenced by regional variations in total POC production and in remineralization length scale, variations in maximum annual MLD remain a dominant influence on the discrepancy among depth horizons (Figure 2). This effect is also evident in comparisons with the seasonal MLD, euphotic depth, and particle compensation depth horizons (Figure S3). Regions with deep winter mixing are therefore locations where the conclusions of both observational and modeling studies are particularly sensitive to the choice of export depth horizon and where the rate of carbon sequestration could be significantly overestimated when using export depth horizons shallower than the maximum annual MLD.

3.3. Global Rates and Spatial Patterns of POC Flux and e-Ratio

To determine how different choices of depth horizon influence our global understanding of export, we calculate the model's global annual mean POC flux and e-ratio using all five depth horizon choices (Table 1). The model's global POC flux is on the low end of observational estimates, yielding rates ranging from 5.3 to 6.9 Pg C/year across the suite of depth horizons considered here. This range reflects a 30% difference in the model's total estimate of global POC flux depending only on the choice of export depth horizon. Modeled global e-ratios similarly vary across different export horizons, with a global e-ratio evaluated at the seasonally varying MLD that is 21% greater than the global mean e-ratio evaluated at the maximum annual MLD. Variations in depth horizon choice cannot explain the full range of

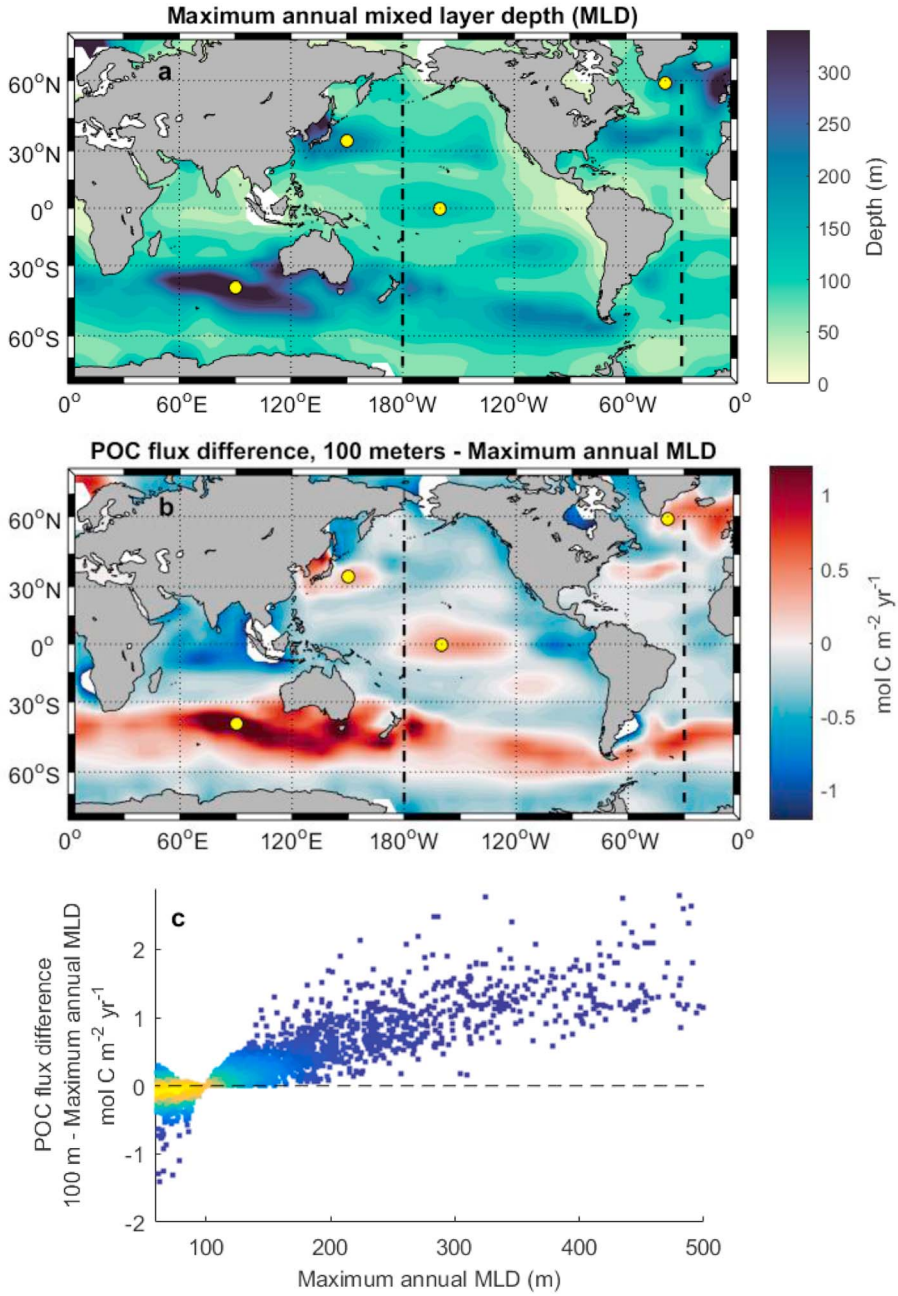

Figure 2. (a) Maximum annual MLD. (b) Difference between POC flux determined at the fixed depth horizon of 100 m and at the maximum annual MLD. (c) Relationship between the maximum annual MLD and the POC flux difference between the fixed 100-m and maximum annual MLD depth horizons, shown spatially in (b), (r^2 = 0.69). Each point represents an individual grid cell, with points where maximum annual MLD <60 m omitted and the colors representing overlapping point density. In (a) and (b), dashed lines show locations of the sections in Figure 1 and yellow dots show the locations highlighted in Figure 3. MLD = mixed layer depth; POC = particulate organic carbon.

observational estimates of global export rates and efficiency (which include a spread representing >100% difference across estimates; Siegel et al., 2016) but can contribute significantly to uncertainty in these global estimates.

Differences in the spatial patterns of POC flux and e-ratio across differing choices of export depth horizon are even more pronounced (Figure 3). For example, there is a strong zonal contrast between high- and

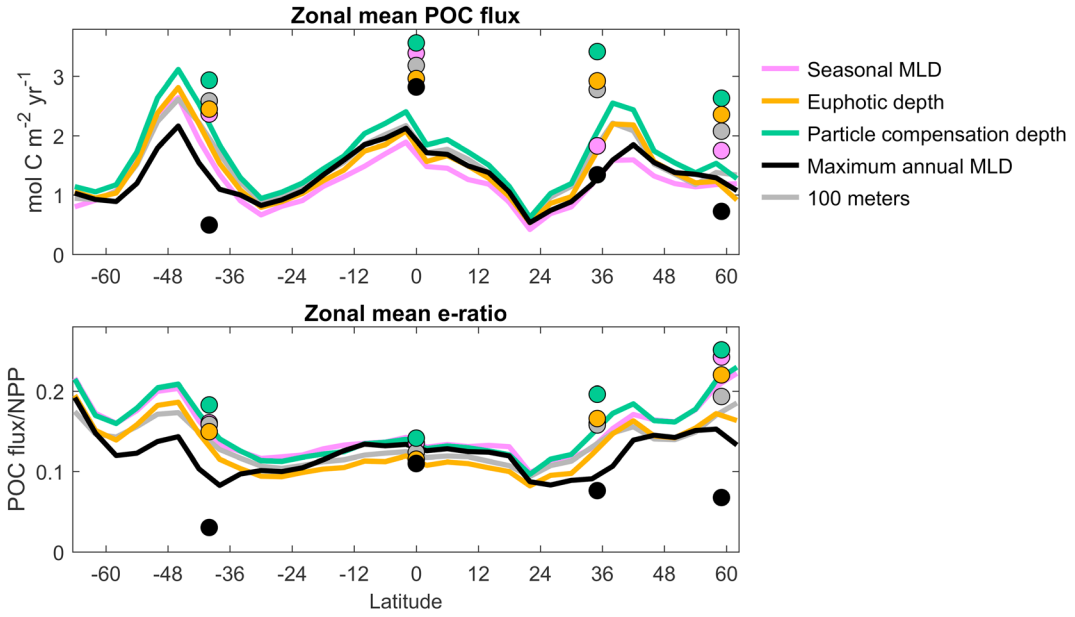

Figure 3. Zonal mean annual POC flux (top) and e-ratio (bottom), evaluated at each of five depth horizons for defining export. Examples of the spread among depth horizons from locations with relatively deep maximum annual MLDs in the Southern Ocean, equatorial Pacific, Kuroshio Extension, and Irminger Sea (shown in map view in Figure 2) are plotted by latitude in the colored circles. MLD = mixed layer depth; POC = particulate organic carbon.

low-latitude POC flux and e-ratios evaluated at the euphotic depth, with 105% higher POC flux and 49% greater e-ratios in the polar and subpolar latitudes (30°N–70°N and 30°S–70°S) than in the subtropics (10°N–30°N and 10°S–30°S). However, the contrast is considerably reduced, to just 58% for POC flux and 8% for e-ratio, when evaluated instead at the maximum annual MLD. This is a result of spatial structure in the variable depth horizons, with the largest discrepancy between depth horizons found at subpolar latitudes where the euphotic and particle compensation depths are shallowest and maximum annual mixed layers are deepest (Figures 1 and 2a). This could at least partially explain the methodological discrepancy in annual export rates previously noted by Emerson (2014) where satellite algorithms and models, which generally use the euphotic depth or 100-m horizons, find greater zonal contrast than mass balance approaches, which generally use the seasonal or maximum annual MLD.

For in situ observational studies comparing export measurements at individual field locations, these differences among export depth horizons can be especially confounding. We compare modeled POC flux and e-ratio across the five depth horizons at four locations representing a range of ocean regions with relatively deep maximum annual MLDs: the Irminger Sea, the Kuroshio Extension, the equatorial Pacific, and the Indian sector of the Southern Ocean (Figure 3; locations shown in map view in Figures 2a and 2b). Within each station, estimates based on different export depth horizons can range widely, with POC flux and e-ratios determined at the particle compensation depth yielding rates that are 1.3–6 times higher than rates determined at the maximum annual MLD. Conclusions of regional differences based on comparisons across stations are also highly sensitive to the choice of export depth horizon. For example, POC flux from the euphotic zone is comparable in the equatorial Pacific and the Kuroshio Extension region of the western North Pacific but export from the seasonally varying MLD and maximum annual MLD are ~2 times greater in the equatorial Pacific than in the Kuroshio Extension (Figure 3a). Similarly, in comparing among the four example stations in Figure 3b, the e-ratio in the equatorial Pacific is the lowest of all stations when evaluated at the euphotic depth but greatest when evaluated at the maximum annual MLD. These discrepancies could be even more pronounced if evaluated over shorter seasonal timescales rather than the full year (Figure S2). This emphasizes the importance of accounting for variations across depth horizon in interpreting observational data to compare among studies and regions.

4. Conclusions and Future Outlook

Using a single dynamically consistent global ocean biogeochemical model, we demonstrate that global rates and spatial patterns of POC flux and e-ratios (the rate and efficiency of export) are sensitive to the choice of depth horizon used to define export (Table 1). Differences among commonly used depth horizons are particularly pronounced in regions that experience deep winter mixing, where POC flux and e-ratios are considerably lower when evaluated at deep maximum annual MLDs than at shallower depth horizons (Figures 2 and 3). This produces much stronger spatial contrast between the high and low latitudes for POC flux and e-ratios evaluated at the euphotic depth or 100 m than when evaluated at the maximum annual MLD (Figure 3), potentially explaining why prior studies using different choices for export depth horizon have reached different conclusions about the spatial variability in global export rates.

Given the range of commonly used choices for export depth horizon, and the strong sensitivity of conclusions about global rates and spatial patterns of POC flux and e-ratio to this choice, we recommend that studies of export rates and efficiency explicitly state how export was defined and discuss the influence of the choice of depth horizon on the results. While a single agreed-upon definition of the depth horizon used to define export would certainly clarify the literature, we do not recommend a single "correct" depth horizon choice because different definitions may be best suited to addressing different scientific questions, in addition to being more practical when using different observational approaches. However, comparisons among studies using varying methods should account for different choices of export depth horizon as a potential reason for discrepancies and endeavor to compare estimates normalized to the same export depth horizon. This is essential not only for studies of POC flux but also observational and model analyses of the contributions of zooplankton vertical transport and DOC flux to export, as mechanisms of physical mixing and active vertical migration will produce vertical patterns of export flux that differ from the POC dynamics explored here (e.g., Roshan & DeVries, 2017; Steinberg & Landry, 2017). To enable intercomparison among studies, export rates and efficiency should be evaluated as profiles across multiple depth horizons wherever possible. For instance, model studies could archive full profiles of POC flux rather than only archiving flux at 100 m (planned for future model intercomparison; Orr et al., 2016) and observational studies that collect depth profiles (e.g., from profiling floats or high-resolution discrete sampling profiles) could report export estimates integrated to multiple depth horizons in addition to publishing the full observational data set to assist in future reanalysis. This is especially important for high-latitude regions with deep winter mixing extending below the euphotic zone, which feature the largest discrepancies in estimated rates and efficiency of export among different depth horizons (Figures 2 and 3). As current and future research programs remedy the historical gap in year-round biogeochemical observations in high-latitude regions (e.g., Johnson et al., 2017; Siegel et al., 2016), attention to evaluating export across multiple depth horizons will be particularly critical.

Acknowledgments
The CCSM-BEC model output used here has all been previously published by Lima et al. (2014). This work was supported by the Postdoctoral Scholar Program at the Woods Hole Oceanographic Institution, with funding provided by the Weston Howland Jr. Postdoctoral Scholarship and by the National Science Foundation (OCE-1434000).

References

Bopp, L., Resplandy, L., Orr, J. C., Doney, S. C., Dunne, J. P., Gehlen, M., et al. (2013). Multiple stressors of ocean ecosystems in the 21st century: Projections with CMIP5 models. *Biogeosciences*, *10*(10), 6225–6245. https://doi.org/10.5194/bg-10-6225-2013

Buesseler, K. O., Antia, A. N., Chen, M., Fowler, S. W., Gardner, W. D., Gustafsson, O., et al. (2007). An assessment of the use of sediment traps for estimating upper ocean particle fluxes. *Journal of Marine Research*, *65*(3), 345–416. https://doi.org/10.1357/002224007781567621

Buesseler, K. O., & Boyd, P. W. (2009). Shedding light on processes that control particle export and flux attenuation in the twilight zone of the open ocean. *Limnology and Oceanography*, *54*(4), 1210–1232. https://doi.org/10.4319/lo.2009.54.4.1210

Buesseler, K. O., Michael, P., Livingston, H. D., & Cochrant, K. (1992). Carbon and nitrogen export during the JGOFS North Atlantic Bloom Experiment estimated from ^{234}Th:^{238}U disequilibria. *Deep Sea Research*, *39*(7), 1115–1137. https://doi.org/10.1016/0198-0149(92)90060-7

DeVries, T., Primeau, F., & Deutsch, C. (2012). The sequestration efficiency of the biological pump. *Geophysical Research Letters*, *39*, L13601. https://doi.org/10.1029/2012GL051963

Doney, S. C., Lima, I., Moore, J. K., Lindsay, K., Behrenfeld, M. J., Westberry, T. K., et al. (2009). Skill metrics for confronting global upper ocean ecosystem-biogeochemistry models against field and remote sensing data. *Journal of Marine Systems*, *76*(1–2), 95–112. https://doi.org/10.1016/j.jmarsys.2008.05.015

Doney, S. C., Lindsay, K., & Moore, J. K. (2003). Global ocean carbon cycle modeling. In M. Fasham (Ed.), *Ocean biogeochemistry* (pp. 217–238). Berlin, Germany: Springer. https://doi.org/10.1007/978-3-642-55844-3_10

Dunne, J. P., Armstrong, R. A., Gnanadesikan, A., & Sarmiento, J. L. (2005). Empirical and mechanistic models for the particle export ratio. *Global Biogeochemical Cycles*, *19*, GB4026. https://doi.org/10.1029/2004GB002390

Dunne, J. P., Sarmiento, J. L., & Gnanadesikan, A. (2007). A synthesis of global particle export from the surface ocean and cycling through the ocean interior and on the seafloor. *Global Biogeochemical Cycles*, *21*, GB4006. https://doi.org/10.1029/2006GB002907

Emerson, S. (2014). Annual net community production and the biological carbon flux in the ocean. *Global Biogeochemical Cycles*, *28*, 14–28. https://doi.org/10.1002/2013GB004680

Emerson, S. R., & Hedges, J. I. (2008). *Chemical oceanography and the marine carbon cycle*. New York: Cambridge University Press. https://doi.org/10.1017/CBO9780511793202

Estapa, M., Durkin, C., Buesseler, K., Johnson, R., & Feen, M. (2017). Carbon flux from bio-optical profiling floats: Calibrating transmissometers for use as optical sediment traps. *Deep Sea Research Part I*, *120*, 100–111. https://doi.org/10.1016/j.dsr.2016.12.003

Estapa, M. L., Siegel, D. A., Buesseler, K. O., Stanley, R. H. R., Lomas, M. W., & Nelson, N. B. (2015). Decoupling of net community and export production in the Sargasso Sea. *Global Biogeochemical Cycles*, *29*, 1266–1282. https://doi.org/10.1002/2014GB004913

Hansell, D. A., & Carlson, C. A. (1998). Net community production of dissolved organic carbon. *Global Biogeochemical Cycles*, *12*(3), 443–453. https://doi.org/10.1029/98GB01928

Henson, S. A., Sanders, R., Madsen, E., Morris, P. J., Le Moigne, F., & Quartly, G. D. (2011). A reduced estimate of the strength of the ocean's biological carbon pump. *Geophysical Research Letters*, *38*, L04606. https://doi.org/10.1029/2011GL046735

Johnson, K. S., Plant, J. N., Coletti, L. J., Jannasch, H. W., Sakamoto, C. M., Riser, S. C., et al. (2017). Biogeochemical sensor performance in the SOCCOM profiling float array. *Journal of Geophysical Research: Oceans*, *122*, 6416–6436. https://doi.org/10.1002/2017JC012838

Körtzinger, A., Send, U., Lampitt, R. S., Hartman, S., Wallace, D. W. R., Karstensen, J., et al. (2008). The seasonal pCO_2 cycle at 49°N/16.5°W in the northeastern Atlantic Ocean and what it tells us about biological productivity. *Journal of Geophysical Research*, *113*, C04020. https://doi.org/10.1029/2007JC004347

Laufkötter, C., Vogt, M., Gruber, N., Aumont, O., Bopp, L., Doney, S. C., et al. (2016). Projected decreases in future marine export production: The role of the carbon flux through the upper ocean ecosystem. *Biogeosciences*, *13*(13), 4023–4047. https://doi.org/10.5194/bg-13-4023-2016

Laws, E., Falkowski, P., Smith, W. J., Ducklow, H., & McCarthy, J. (2000). Temperature effects on export production in the open ocean. *Global Biogeochemical Cycles*, *14*(4), 1231–1246. https://doi.org/10.1029/1999GB001229

Laws, E. A., D'Sa, E., & Naik, P. (2011). Simple equations to estimate ratios of new or export production to total production from satellite-derived estimates of sea surface temperature and primary production. *Limnology and Oceanography: Methods*, *9*(12), 593–601. https://doi.org/10.4319/lom.2011.9.593

Lima, I. D., Lam, P. J., & Doney, S. C. (2014). Dynamics of particulate organic carbon flux in a global ocean model. *Biogeosciences*, *11*(4), 1177–1198. https://doi.org/10.5194/bg-11-1177-2014

Marsay, C. M., Sanders, R. J., Henson, S. A., Pabortsava, K., Achterberg, E. P., & Lampitt, R. S. (2015). Attenuation of sinking particulate organic carbon flux through the mesopelagic ocean. *Proceedings of the National Academy of Sciences of the United States of America*, *112*(4), 1089–1094. https://doi.org/10.1073/pnas.1415311112

Martin, J. M., Knauer, G. A., Karl, D. M., & Broenkow, W. W. (1987). VERTEX: Carbon cycling in the Northeast Pacific. *Deep Sea Research*, *34*(2), 267–285. https://doi.org/10.1016/0198-0149(87)90086-0

Moore, J. K., Doney, S. C., & Lindsay, K. (2004). Upper ocean ecosystem dynamics and iron cycling in a global three-dimensional model. *Global Biogeochemical Cycles*, *18*, GB4028. https://doi.org/10.1029/2004GB002220

Najjar, R. G., Jin, X., Louanchi, F., Aumont, O., Caldeira, K., Doney, S. C., et al. (2007). Impact of circulation on export production, dissolved organic matter, and dissolved oxygen in the ocean: Results from Phase II of the Ocean Carbon-Cycle Model Intercomparison Project (OCMIP-2). *Global Biogeochemical Cycles*, *21*, GB3007. https://doi.org/10.1029/2006GB002857

Najjar, R. G., & Keeling, R. F. (1997). Analysis of the mean annual cycle of the dissolved oxygen anomaly in the World Ocean. *Journal of Marine Research*, *55*(1), 117–151. https://doi.org/10.1357/0022240973224481

Orr, J. C., Najjar, R. G., Aumount, O., Bopp, L., Bullister, J. L., Danabasoglu, G., et al. (2016). Biogeochemical protocols and diagnostics for the CMIP6 Ocean Model Intercomparison Project (OMIP). *Geoscientific Model Development Discussion*, *0*, 1–45. https://doi.org/10.5194/gmd-2016-155

Palevsky, H. I., Quay, P. D., Lockwood, D. E., & Nicholson, D. P. (2016). The annual cycle of gross primary production, net community production, and export efficiency across the North Pacific Ocean. *Global Biogeochemical Cycles*, *30*, 361–380. https://doi.org/10.1002/2015GB005318

Palevsky, H. I., Quay, P. D., & Nicholson, D. P. (2016). Discrepant estimates of primary and export production from satellite algorithms, a biogeochemical model, and geochemical tracer measurements in the North Pacific Ocean. *Geophysical Research Letters*, *43*, 8645–8653. https://doi.org/10.1002/2016GL070226

Roshan, S., & DeVries, T. (2017). Efficient dissolved organic carbon production and export in the oligotrophic ocean. *Nature Communications*, *8*(1), 2036. https://doi.org/10.1038/s41467-017-02227-3

Siegel, D. A., Buesseler, K. O., Behrenfeld, M. J., Benitez-Nelson, C. R., Boss, E., Brzezinski, M. A., et al. (2016). Prediction of the export and fate of global ocean net primary production: The EXPORTS science plan. *Frontiers in Marine Science*, *3*(22). https://doi.org/10.3389/fmars.2016.00022

Siegel, D. A., Buesseler, K. O., Doney, S. C., Sailley, S. F., Behrenfeld, M. J., & Boyd, P. W. (2014). Global assessment of ocean carbon export by combining satellite observations and food-web models. *Global Biogeochemical Cycles*, *28*, 181–196. https://doi.org/10.1002/2013GB004743

Stange, P., Bach, L. T., Le Moigne, F. A. C., Taucher, J., Boxhammer, T., & Riebesell, U. (2017). Quantifying the time lag between organic matter production and export in the surface ocean: Implications for estimates of export efficiency. *Geophysical Research Letters*, *44*, 268–276. https://doi.org/10.1002/2016GL070875

Steinberg, D. K., Carlson, C. A., Bates, N. R., Goldthwait, S. A., Madin, L. P., & Michaels, A. F. (2000). Zooplankton vertical migration and the active transport of dissolved organic and inorganic carbon in the Sargasso Sea. *Deep Sea Research Part I: Oceanographic Research Papers*, *47*(1), 137–158. https://doi.org/10.1016/S0967-0637(99)00052-7

Steinberg, D. K., & Landry, M. R. (2017). Zooplankton and the ocean carbon cycle. *Annual Review of Marine Science*, *9*(1), 413–444. https://doi.org/10.1146/annurev-marine-010814-015924

Taylor, K. E., Stouffer, R. J., & Meehl, G. A. (2012). An overview of CMIP5 and the experiment design. *Bulletin of the American Meteorological Society*, *93*(4), 485–498. https://doi.org/10.1175/BAMS-D-11-00094.1